Received: Added at production | Revised: Added at production | Accepted: Added at production

DOI: xxx/xxxx

RESEARCH ARTICLE

Attitude Determination for Multirotor Aerial Vehicles using a Predefined-time Super Twisting Algorithm

João Filipe Silva* | Davi A. Santos

Department of Mechatronics, Aeronautics Institute of Technology (ITA), São Paulo, Brazil

Correspondence
*João Filipe Silva, Department of Mechatronics, Aeronautics Institute of Technology (ITA), São José dos Campos, São Paulo, 12228-900, Brazil.
Email: joaofilipe@ita.br

Funding Information
This research was supported by the Conselho Nacional de Desenvolvimento Científico e Tecnológico, Grant/Award Numbers: 141524/2020-0 and 304300/2021-7; Financiadora de Estudos e Projetos, Grant/Award Number: 01.22.0069.00.

Abstract

In recent works, well-known three-dimensional localization methods studied in the aerospace field have been revisited for applications on multirotor aerial vehicles (MAVs). However, most of these classic methods employ stochastic estimators that are asymptotically stable, in a stochastic sense, and exhibit high sensitivity to disturbances and model uncertainties. The goal of this paper is to propose and evaluate a novel solution to the localization problem of MAVs, employing multivariable robust observers based on sliding-mode techniques. Aiming to improve on the existing methods usually based on the extended Kalman filter, this paper investigates sliding-mode techniques to reach finite-time stabilization of the estimation error and provide robustness to disturbances and uncertainties. The super-twisting algorithm (STA) is considered as a starting point for its recognized performance when used to design differentiators. In particular, a modification of the STA is proposed, replacing one of its terms with a certain time-varying function that allows the upper bound of the settling time of the resulting algorithm to be a direct adjustable parameter. The proposed algorithm's behavior is numerically evaluated and is shown to yield the predicted properties even in the presence of bounded disturbances and uncertainties. Additionally, an attitude determination problem employing the proposed algorithm is presented as an application. The three-dimensional attitude and angular velocity of an MAV are accurately estimated under strict settling-time restrictions, using only the vector measurements provided by an accelerometer and a magnetometer.

KEYWORDS:
Super-twisting algorithm, Predefined convergence time, Attitude determination

1 | INTRODUCTION

In the last three decades, the super-twisting algorithm (STA)[1,2] has been widely applied to the design of finite-time robust state estimators for mechanical systems[3,4] and, in particular, for three-axis attitude kinematics[5,6]. Recent extensions of the classical STA have been developed to provide it with fixed-time stability (FxTS)[7,8] or prescribed-time stability (PTS)[9], which allow the bound of the settling time to be adjustable independent of the initial conditions. This new characteristic has an immediate practical impact on the performance tweaking of state observers, from which an attitude determination system can benefit. An example is the need for an accurate attitude estimate of a multirotor aerial vehicle (MAV) before a mission measurement or manipulation can be carried out.

The use of the STA in applications involving a bound requirement on the convergence time is not immediate since there is no explicit and straightforward relationship between its settling-time bound and its parameters. In fact, the available settling-time estimates obtained via Lyapunov analysis turn out to be very conservative [10,11], while the one obtained from a recent analytical solution to the STA is considerably complex to compute [12]. Moreover, a global finite upper bound for the settling time (UBST) cannot be obtained for the conventional STA since the actual settling time itself increases indefinitely as the initial conditions go to infinity. Cruz et *al.* [13] have modified the STA to endow it with the FxTS property, thus allowing the derivation of a finite UBST that is uniform in the initial condition. However, that UBST is also too conservative to be used as an estimate of the actual settling time, while also presenting a complicated relation with the system's parameters. To address both issues, Seeber et *al.* [14] proposed a gain-tuning method to guarantee convergence of the fixed-time STA [13] within a specified UBST. Nevertheless, no STA-like algorithm that converges exactly at a directly specified instant has appeared in the literature yet.

The three-axis attitude determination from vector observations [15] has been extensively investigated in the aerospace literature since the 1960s [16–25]. It consists of estimating the three-dimensional attitude of a body using measurements of non-collinear geometric vectors taken in a body-fixed Cartesian coordinate system (CCS) as well as in a reference CCS. Attitude determination methods can be static or dynamic [26]. The former ones do not consider the attitude variation over time, thus being able to only process the present measures for estimating the present attitude [15–17,26]. The QUEST algorithm [17] is a classic example in this class; it provides a least-square estimate of the body's attitude quaternion using measurements of two or more non-collinear vectors in a batch procedure. The dynamic methods, in turn, require knowledge of the body's motion for assimilating information of the past estimates into the present one. In this case, if the suite of sensors contains a three-axis rate-gyro, the body's motion can be acquired from the kinematic equation and the provided angular velocity measures, which enter the kinematic equation as known forcing inputs [20–25]. It turns out, however, that those measures contain drifting biases, which must be jointly estimated to achieve high precision in the attitude estimation. Otherwise, if a rate-gyro is not available, the angular velocity must also be estimated to completely acquire the body's motion, which requires the use of the attitude dynamic equation along with the kinematic one [27–33]. A relevant issue found here is that the attitude dynamic equation usually involves unknown disturbances (e.g., wind) and uncertainties (e.g., in the inertia parameters), which also negatively impact the overall estimation performance.

The classic attitude determination methods can be directly applied to MAVs equipped with an accelerometer and a magnetometer [34,35]. Furthermore, a dynamic attitude estimation method is required, since the flight control routines require a feedback of the vehicle's rotational states. A plethora of dynamic methods has been recently reported in the MAV literature, such as complementary filters [34–38], Kalman filters [39–43], and high-gain observers [44]. None of the aforementioned methods provides robust error convergence, which is desirable in gyroless applications to deal with the uncertainties in the dynamic equation. Contrarily, estimators based on robust high-order sliding-mode observers [45–48] and, particularly, on the conventional STA [5,6] have also been reported, but do not consider a strict convergence time restriction.

To fill the aforementioned gaps, the present paper proposes a modification of the conventional super-twisting algorithm, which presents robust finite-time stability with convergence of its states to the origin at a predefined instant. Different from the works in predefined-time stability [9,49–51], our proposed algorithm uses both a time-varying and a switching gain, to provide robustness and the desired convergence performance. With respect to three-axis attitude determination without rate-gyro measurements, our proposed two-step solution enables the explicit tuning of the estimation error convergence instant, different from the aforementioned works in which this instant was not finite [42] or was conservatively estimated [5,6]. First, the QUEST algorithm is employed to calculate an optimal attitude estimate from the accelerometer and magnetometer measurements. Then, the determined attitude is directly used as an input for the state observer, formulated from the previously proposed algorithm. While most of the literature in gyroless dynamic attitude determination rely on the estimation of the disturbances to compensate for their effect [27–33], our proposed observer provides estimates of attitude and its derivative that robustly converge to the actual states in predefined time. In summary, the contributions of this paper are:

- A novel second-order sliding-mode algorithm that guarantees finite-time stability with a predefined convergence time.
- The application of the proposed algorithm to the robust attitude determination problem for a flying vehicle, without the use of rate-gyro measurements.

In the following, Section 2 presents the mathematical preliminaries required to introduce the proposed results. Section 3 contains the proposed modified super-twisting algorithm, as well as a geometric analysis that proves the existence of system parameters that guarantee the predefined-time attractiveness of the origin. A sliding-mode observer-based solution to the robust attitude determination problem, without the use of rate-gyro measurements, is provided Section 4 as an evaluation of the proposed algorithm's efficacy. Finally, Sections 5 and 6 present the simulation results and the conclusions of this paper, respectively.

2 | PRELIMINARIES

This section presents an analysis of the properties of a first-order system formulated from a polynomial function with predefined convergence time, followed by the description of the conventional STA in its SISO and MIMO formulations.

2.1 | First-order system with predefined convergence time

Consider a polynomial time function $\pi : \mathbb{R}_{\geq t_0} \to \mathbb{R}$, with initial instant $t_0 \in \mathbb{R}_{\geq 0}$, defined as

$$\pi(t) = \pi(t_0)\left(\frac{t_c - t}{t_c - t_0}\right)^{\eta}, \tag{1}$$

where $t \in \mathbb{R}_{\geq t_0}$ represents the current instant of time, $\eta \in \mathbb{Z}_{\geq 1}$ is a constant exponent, and $t_c \in \mathbb{R}_{>t_0}$ is the predefined convergence instant.

The following lemma summarizes the converging properties of π in the time interval $[t_0, t_c]$, as t approaches t_c from the left.

Lemma 1. It holds that

(i). $\pi(t_c) = 0$,

(ii). π is continuous in all its domain $\mathbb{R}_{\geq 0}$,

(iii). if $\pi(t_0) > 0$, $\pi(t)$ is strictly decreasing in $[t_0, t_c) \subset \mathbb{R}$,

(iv). if $\pi(t_0) < 0$, $\pi(t)$ is strictly increasing in $[t_0, t_c) \subset \mathbb{R}$.

Proof. Item *(i)* can be immediately verified by replacing $t = t_c$ into (1). To show item *(ii)*, note that every polynomial function is continuous everywhere. Therefore, since π is polynomial, it is continuous in all its domain $\mathbb{R}_{\geq t_0}$. Now, by taking the first derivative of (1) with respect to t, we obtain

$$\dot{\pi}(t) = -\frac{\eta\pi(t_0)}{t_c - t_0}\left(\frac{t_c - t}{t_c - t_0}\right)^{\eta-1}, \quad \forall t \in \mathbb{R}_{\geq t_0}.$$

Since $(t_c - t) > 0$, $\forall t \in [t_0, t_c)$, for any $\pi(t_0) > 0$, it holds that $\dot{\pi}(t) < 0$, $\forall t \in [t_0, t_c)$, thus showing item *(iii)*. Similarly, for any $\pi(t_0) < 0$, it holds that $\dot{\pi}(t) > 0$, $\forall t \in [t_0, t_c)$, which proves item *(iv)*. □

Based on Lemma 1, we can affirm that, independent of the initial condition $\pi(t_0)$, in the time interval $[t_0, t_c]$, the function π always converges to 0 as t approaches t_c from the left. Moreover, since $\dot{\pi}$ does not change its sign in $[t_0, t_c]$, that convergence occurs in a monotonic manner, *i.e.*, without oscillating.

Function $\pi(t)$ has interesting convergence properties in the time interval $[t_0, t_c]$, but, after $t = t_c$, we can immediately verify that it does not keep at 0. Since we are rather interested in a function of time that converges to zero at a specified instant t_c and keeps there forever, now, let us consider the following modified function:

$$\varpi(t) = \varpi_0\left(\frac{t_c - t}{t_c - t_0}\right)^{\eta} \mathbb{I}_{[t_0,t_c)}(t), \tag{2}$$

where $\varpi_0 \triangleq \varpi(t_0)$, and $\mathbb{I}_{[t_0,t_c)}(t)$ is an indicator function of the time interval $[t_0, t_c)$, *i.e.*, $\mathbb{I}_{[t_0,t_c)}(t) = 1, \forall t \in [t_0, t_c)$, and $\mathbb{I}_{[t_0,t_c)}(t) = 0, \forall t \in [t_c, \infty)$.

The following lemma addresses the smoothness of the modified function ϖ at $t = t_0 + \tau_c$.

Lemma 2. Consider a positive integer $n < \eta$. It holds that ϖ is nth-order differentiable in $\mathbb{R}_{>t_0}$.

Proof. In both intervals $[t_0, t_c)$ and $[t_c, \infty)$, the function ϖ is polynomial and, therefore, it is differentiable of an arbitrary order. It remains to analyze its differentiability at $t = t_c$. On the one hand, the right nth-order semi-derivative of ϖ at $t = t_c$ is clearly $\varpi_+^{(n)}(t_c) = 0$.

On the other hand, to evaluate its left nth-order semi-derivative at the same point, let us first obtain it in the time interval $[t_0, t_c)$ as

$$\varpi_{-}^{(n)}(t) = (-1)^n \frac{\eta!}{(\eta-n)!} \frac{\varpi_0}{(t_c - t_0)^n} \left(\frac{t_c - t}{t_c - t_0}\right)^{\eta-n}, \quad \forall t \in [t_0, t_c).$$

From the expression above, if $\eta = n$ or $\eta < n$, we have $\varpi_{-}^{(n)}(t_c) = (-1)^n n! \varpi_0 (t_c - t_0)^{-n}$ or $\varpi_{-}^{(n)}(t_c) = \pm\infty$, respectively. However, under the condition $\eta > n$, it is computed as $\varpi_{-}^{(n)}(t_c) = 0$, thus agreeing with its right counterpart, which implies the nth-order differentiability of ϖ at $t = t_c$. This completes the proof. □

From the previous lemma, we see that ϖ can be made arbitrarily smooth in all its domain (and, in particular, at instant $t = t_c$) by just choosing the integer exponent η to be larger than the derivative order n. Particularly, note that if $\eta = 1$, $\varpi(t)$ is not smooth at $t = t_c$, although it is continuous there (see Figure 1). To verify, note that it is immediate to check that the right limit of ϖ at $t = t_c$ is zero and, on the other hand, we can also compute the left limit as zero:

$$\lim_{t \to t_c^-} \varpi(t) = \lim_{t \to t_c^-} \varpi_0 \left(\frac{t_c - t}{t_c - t_0}\right) = 0. \tag{3}$$

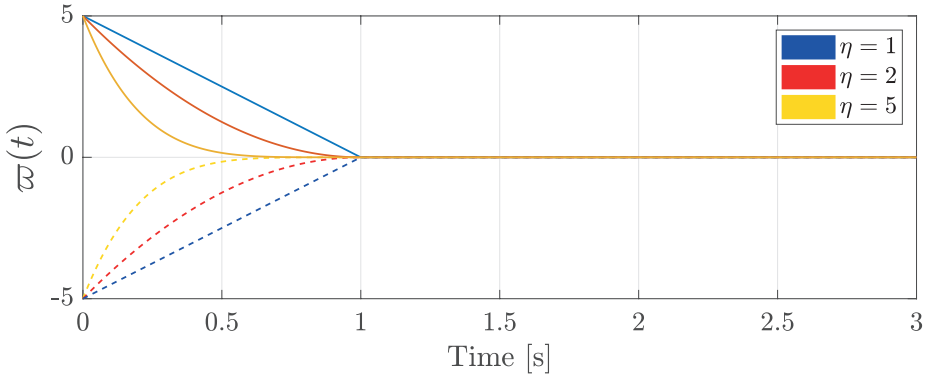

Figure 1: Smoothness analysis of $\varpi(t)$ at $t = t_c$, for $t_0 = 0$, $t_c = 1$, and $|\varpi(0)| = 5$.

From the proof of Lemma 2, we can extract the following formula for the nth-order time derivative of $\varpi(t)$

$$\varpi^{(n)}(t) = (-1)^n \frac{\eta!}{(\eta-n)!} \frac{\varpi_0}{(t_c - t_0)^n} \left(\frac{t_c - t}{t_c - t_0}\right)^{\eta-n} \mathbb{I}_{[t_a, t_c)}(t), \tag{4}$$

for $n < \eta$.

Now, for convenience, consider the following initial value problem (IVP):

$$\dot{x}(t) = f(t, x; \Omega), \quad x(t_0) \triangleq x_0 \in \mathbb{R}, \quad t \in \mathbb{R}_{\geq t_0}, \tag{5}$$

where $x(t) \in \mathcal{D} \subseteq \mathbb{R}^n$, with $0 \in \mathcal{D}$, $t_0 \in \mathbb{R}_{\geq 0}$ is the initial time, $\Omega \in \mathbb{R}^m$ is the vector containing the constant parameters of the system, and $f : \mathbb{R}_{\geq 0} \times \mathcal{D} \to \mathbb{R}^n$ is a nonlinear function such that $f(\cdot, \cdot)$ is jointly continuous in t and x, and $f(t, 0) = 0$, $\forall t \in [t_0, \infty)$. Consider that f is given by

$$f(t, x; \Omega) \triangleq \begin{cases} -\frac{\eta}{t_c - t} x, & t \in [t_0, t_c), \\ 0, & t \in [t_c, \infty), \end{cases} \tag{6}$$

with $\Omega \triangleq (\eta, t_c)$, $t_c \in \mathbb{R}_{>t_0}$ and $\eta \in \mathbb{Z}_{\geq 1}$.

A solution to (5), which we denote by $x(t; t_0, x_0)$, is understood as a first-order differentiable function that satisfies the ODE $\dot{x} = f(t, x)$ and the initial condition, *i.e.*, $x(t_0; t_0, x_0) = x_0$.

Proposition 1. The IVP in (5)–(6) has a unique solution in $t \in [t_0, \infty)$ given by

$$x(t; t_0, x_0) = x_0 \left(\frac{t_c - t}{t_c - t_0}\right)^{\eta} \mathbb{I}_{[t_0, t_c)}(t). \tag{7}$$

Proof. Suppose (7) is a solution to (5)–(6). By differentiating (7) with respect to time, we obtain:

$$\dot{x}(t;t_0,x_0) = -\frac{\eta x_0}{(t_c-t_0)^\eta}\left(t_c-t\right)^{\eta-1}\mathbb{I}_{[t_0,t_c)}(t). \tag{8}$$

By substituting (7) and (10) into (5), we obtain an identity for all $t \in \mathbb{R}_{\geq t_0}$, thus proving that (7) is indeed a solution to (5). Now, to prove uniqueness, suppose that there exists another solution and, without loss of generality, let us write it as

$$\nu(t;t_0,x_0) = x(t;t_0,x_0) + \phi(t), \tag{9}$$

where ϕ is differentiable for $\nu(t;t_0,x_0)$ to also be. Therefore, by replacing (9) and its derivative into (5), we obtain:

$$\dot{x}(t;t_0,x_0) + \dot{\phi}(t) = \begin{cases} -\frac{\eta}{t_c-t}\left(x(t;t_0,x_0)+\phi(t)\right), & t \in [t_0,t_c), \\ 0, & t \in [t_c,\infty). \end{cases} \tag{10}$$

Since (7) is a solution to (5), we can write

$$\dot{x}(t;t_0,x_0) = \begin{cases} -\frac{\eta}{t_c-t}x(t;t_0,x_0), & t \in [t_0,t_c), \\ 0, & t \in [t_c,\infty). \end{cases} \tag{11}$$

By substituting (11) into (10), we obtain:

$$\dot{\phi}(t) = \begin{cases} -\frac{\eta}{t_c-t}\phi(t), & t \in [t_0,t_c), \\ 0, & t \in [t_c,\infty). \end{cases} \tag{12}$$

From the Peano's Theorem (see[52], p.10), we know that there is at most one solution to (5)–(6) on $t \in [t_0,t_c)$. On the other hand, from (12), we have $\dot{\phi}(t) = 0,\ t \in [t_c,\infty)$. Furthermore, since the solution is unique for $t \in [t_0,t_c)$, ϕ is continuous, and because $x(t,t_0,x_0) \to 0$ as $t \to t_c^-$, it is true that $\phi(t_c) = 0$. Therefore, we have that $\phi(t) = 0, \forall t \geq t_c$, which implies that the solution is unique on $[t_c,\infty)$ as well. □

Additionally, the following lemma states the predefined-time attractiveness of the origin of a disturbed system like (5)–(6).

Lemma 3. Consider the nonautonomous system in (5) with f given by

$$f(t,x;\Omega) \triangleq \begin{cases} -\frac{n}{t_c-t}x(t) + \delta(t), & t \in [t_0,t_c), \\ 0, & t \in [t_c,\infty), \end{cases} \tag{13}$$

where $\delta : \mathbb{R}_{\geq 0} \to \mathbb{R}^n$ is a bounded disturbance, with $|\delta(t)| \leq L$ and L is a positive finite known constant. For $\eta \geq 2$, $x(t)$ converges to zero at the predefined instant t_c.

Proof. The analytic solution of (13), for $t \in [t_0,t_c)$, is given by:

$$x(t) = \left(t_c-t\right)^\eta\left(\int \delta(\tau)\left(t_c-\tau\right)^{-\eta}\,d\tau + c\right). \tag{14}$$

By evaluating the disturbance as a constant signal at its minimum and maximum values, the solution will be bounded as follows:

$$c_1\left(t_c-t\right)^\eta - L\frac{\left(t_c-t\right)}{\eta-1} \leq\ x(t) \leq c_2\left(t_c-t\right)^\eta + L\frac{\left(t_c-t\right)}{\eta-1}, \tag{15}$$

where $-\infty < c_1 \leq \left(\frac{x(t_0)}{(t_c-t_0)^\eta} + \frac{L}{(\eta-1)(t_c-t_0)^{\eta-1}}\right)$ and $\infty > c_2 \geq \left(\frac{x(t_0)}{(t_c-t_0)^\eta} - \frac{L}{(\eta-1)(t_c-t_0)^{\eta-1}}\right)$.

Since, for $\eta \geq 2$, both bounds of the inequality (15) approach zero as $t \to t_c^-$, so will the state $x(t)$. □

2.2 | Super-twisting algorithm

The super-twisting algorithm can be described by[2]

$$\dot{\theta}_1 = -\kappa_1|\theta_1|^{1/2}\,\mathrm{sign}(\theta_1) + \theta_2, \tag{16}$$

$$\dot{\theta}_2 = -\kappa_2\,\mathrm{sign}(\theta_1) + \delta, \tag{17}$$

where $\theta \triangleq (\theta_1,\theta_2) \in \mathbb{R}^2$ is its state vector, $\kappa_1,\kappa_2 > 0$ are design scalar parameters, and $\delta \in \mathbb{R}$ a unknown, but bounded, disturbance signal. In order to extend its application to multi-input systems, it is necessary to substitute the signum function for a

suitable multivariable version. Here, similarly to reported in Nagesh and Edwards[53], the unit-vector approach will be considered, altering equations (16)–(17) to their multivariable version given by

$$\dot{\boldsymbol{\theta}}_1 = -\kappa_1 \frac{\boldsymbol{\theta}_1}{\|\boldsymbol{\theta}_1\|^{1/2}} + \boldsymbol{\theta}_2, \tag{18}$$

$$\dot{\boldsymbol{\theta}}_2 = -\kappa_2 \frac{\boldsymbol{\theta}_1}{\|\boldsymbol{\theta}_1\|} + \boldsymbol{\delta}, \tag{19}$$

where $\boldsymbol{\theta}_1 \in \mathbb{R}^n$, $\boldsymbol{\theta}_2 \in \mathbb{R}^n$, and $\boldsymbol{\delta} \in \mathbb{R}^n$ are now states and disturbance vectors, respectively. As the differential equations in (16)–(19) have discontinuous right hand sides, their solutions must be understood in the Filippov sense[54].

The provided finite-time stable system with predefined convergence time in (5)–(6) is of first order and, therefore, cannot be used to design a differentiator in the same was as the STA. For this reason, the main purpose of this paper is to propose an STA-like finite-time stable system with a predefined convergence time based on system (5)–(6), as well as to construct a second-order sliding-mode observer based on the proposed structure to solve an attitude determination problem.

3 | MODIFIED SUPER-TWISTING ALGORITHM WITH PREDEFINED CONVERGENCE TIME

It is well known that $\dot{\xi} = -|\xi|^{1/2}\,\mathrm{sign}\,(\xi)$ is a first-order finite-time stabilizing function[55]. For the proposed modified algorithm, the first term in the right-hand side of (16) is replaced by a function:

$$\sigma(t,x) \triangleq \begin{cases} \frac{\eta}{t_c - t} x_1(t), & t \in [t_0, t_c), \\ \kappa_1 |x_1(t)|^{1/2}\,\mathrm{sign}\left(x_1(t)\right), & t \in [t_c, \infty). \end{cases} \tag{20}$$

By doing so, the proposed system recovers the conventional STA behavior for all $t \geq t_c$. Therefore, the obtained dynamic system for the modified super-twisting algorithm is given by

$$\dot{x}_1(t) = -\sigma(t,x) + x_2(t), \tag{21}$$

$$\dot{x}_2(t) = -\kappa_2\,\mathrm{sign}\left(x_1(t)\right) + \delta(t), \tag{22}$$

where $\sigma(t,x)$ is given by (20).

Since the conventional STA is known to be finite-time stable, it is necessary to investigate the performance of the system in (21)–(22) during the specified time interval. Consider, from this moment forward, the unperturbed case of system (21)–(22), *i.e.* $\delta = 0,\ \forall t \in \mathbb{R}_{\geq 0}$. The following theorem describes the behavior of $\mathbf{x}(t)$, for $t \in [t_0, t_c)$.

Theorem 1. Denote by $\mathbf{x}(t)$ the solution of system (21)–(22) on $t \in [t_j, t_{j+1})$, where $j = \{0,\ 1,\ 2,\ \dots\}$, and $t_0 < t_1 < \cdots < t_c$. Define the instant t_{j+1} as

$$t_{j+1} = \left\{ \zeta > t_j \ :\ \lim_{t \to \zeta^-} x_1(t) = 0 \right\}.$$

The solution to the IVP (21)–(22), in $t \in [t_j, t_{j+1})$, is given by

$$x_1(t) = \frac{t_c - t}{(\eta-2)(\eta-1)} \left[\mathrm{sign}\left(x_1(t_j)\right)\left[\kappa_2(t_c - t - (\eta-2)(t-t_j))\right] + (\eta-2)x_2(t_j)\right] + \alpha(t_j)\left(\frac{t_c - t}{t_c - t_j}\right)^{\eta}, \tag{23}$$

$$x_2(t) = x_2(t_j) - \kappa_2\,\mathrm{sign}(x_1(t_j))\left[t - t_j\right], \tag{24}$$

where

$$\alpha(t_j) = x_1(t_j) - \frac{\left(t_c - t_j\right)\left[x_2(t_j)(\eta-2) + \mathrm{sign}(x_1(t_j))\kappa_2(t_c - t_j)\right]}{(\eta-2)(\eta-1)}. \tag{25}$$

Proof. Consider equation (22). By the definition in the theorem statement, t_1 is the instant that $x_1(t)$ crosses the zero axis and, consequently, $\mathrm{sign}(x_1(t))$ switches signal. Therefore, $\mathrm{sign}(x_1(t_j))$ remains constant for all $t \in [t_j, t_{j+1})$. Hence, the analytic

solution of (22) in the interval $t \in [t_j, t_{j+1})$ is given by

$$\begin{aligned} x_2(t) &= -\int_{t_j}^{t} \kappa_2 \operatorname{sign}(x_1(t_j))\, d\tau, \\ x_2(t) &= x_2(t_j) - \kappa_2 \operatorname{sign}(x_1(t_j)) \left[t - t_j\right]. \end{aligned} \tag{26}$$

By substituting (26) and (20) in (21), one obtains

$$\dot{x}_1(t) = -\frac{\eta}{t_c - t} x_1(t) + x_2(t_j) - \kappa_2 \operatorname{sign}(x_1(t_j)) \left[t - t_j\right]. \tag{27}$$

Based on the aforementioned assumption that $\operatorname{sign}(x_1(t_j))$ remains constant for all $t \in [t_j, t_{j+1})$, by direct integration one obtains

$$x_1(t) = \frac{t_c - t}{(\eta - 2)(\eta - 1)} \left[\operatorname{sign}\left(x_1(t_j)\right) \left[\kappa_2(t_c - t - (\eta - 2)(t - t_j))\right] + (\eta - 2)x_2(t_j)\right] + \alpha \left(\frac{t_c - t}{t_c - t_j}\right)^{\eta}, \tag{28}$$

$$\alpha(t_j) = x_1(t_j) - \frac{\left(t_c - t_j\right) \left[x_2(t_j)(\eta - 2) + \operatorname{sign}(x_1(t_j))\kappa_2(t_c - t_j)\right]}{(\eta - 2)(\eta - 1)}, \tag{29}$$

thus concluding the proof. □

Figure 2 verifies the analytic solution (23)–(24) by comparing it with the corresponding numerical solution of (21)–(22).

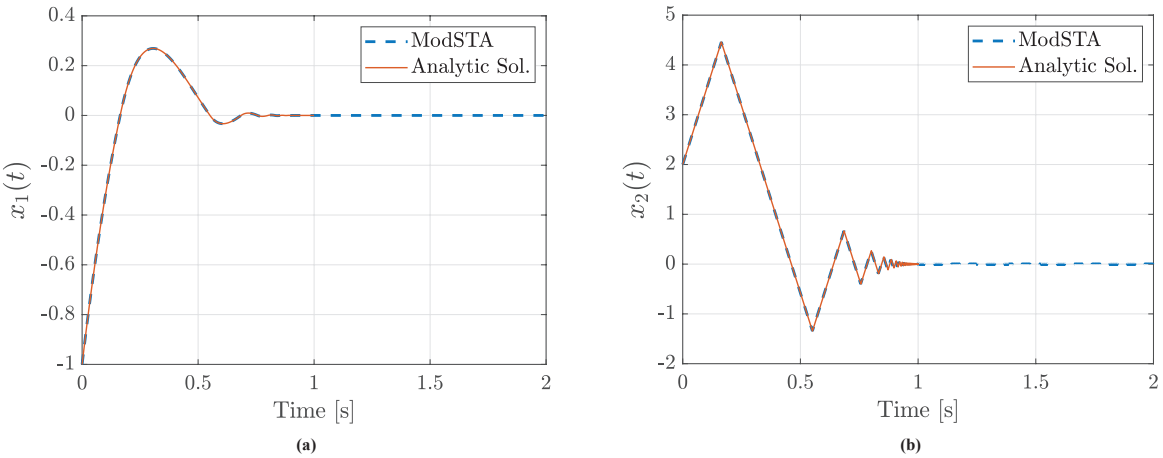

Figure 2: A comparison between the proposed modified STA and its analytic solution, for $t \in [t_0, t_c)$, assuming $\Omega \triangleq \left(\kappa_1,\, \kappa_2,\, \eta,\, t_c\right) = (2,\, 15,\, 6,\, 1\text{s})$.

Corollary 1. For $t \in [t_0, t_c)$, the state x_1 of the unperturbed system (21)–(22) will converge to zero at exactly the predefined instant t_c.

Proof. From (24), for any finite time interval, $x_2(t)$ will only assume infinite values if $|x_2(t_0)| = \infty$ or $\kappa_2 = \infty$. For any other finite values of $|x_2(t_0)|$ and κ_2, $x_2(t)$ will remain bounded. Therefore, from (23), for any $\eta \geq 3$, $x_1(t)$ approaches zero as t approaches t_c. □

Remark 1. The convergence of the state x_2 to zero at $t = t_c$ is not as straightforward to verify, but can be guaranteed with the proper choice of the parameters η and κ_2, as the next theorem will demonstrate.

Corollary 2. The unperturbed system (21)–(22) is finite-time stable.

Proof. From the proof of Corollary 1, by assuming that the initial states and switching gain are finite and by choosing $\eta \geq 3$, the proposed algorithm can be seen as a maneuverer for the conventional STA, delivering to it a vector of initial conditions

$x(t_c) = \left[0\ x_2(t_c)\right]$. Therefore, by satisfying the gain conditions for the stability of the conventional STA[2,56], the states will converge to the origin in finite-time and remain there afterwards. □

The following theorem demonstrates the existence of sufficient parameters to guarantee the predefined convergence time of the state vector to the origin of system (21)–(22), when $\delta(t) = 0$.

Theorem 2. Assume that the initial states of the system are known a priori and consider a set $\mathcal{X} = \left\{\left(t, x_2(t)\right) \mid -\kappa_2\left(t_c - t\right) \leq x_2(t) \leq \kappa_2\left(t_c - t\right)\right\}$. Denote this set as the predefined-time convergence (PTC) area. It is possible to tune the convergence rate η and the switching gain κ_2 to guarantee that $\left(t, x_2(t)\right) \in \mathcal{X}$, $\forall t \in [t_0, t_c)$.

Proof. Consider the known initial condition $x_2(t_0) \neq 0$. From the line segments that delimit the set $\mathcal{X}$, it is possible to see that by choosing a value of κ_2 that satisfies

$$\kappa_2(t_c - t_0) \geq |x_2(t_0)|, \tag{30}$$

the pair $\left(t_0, x_2(t_0)\right)$ will belong to $\mathcal{X}$.

The next step is to ensure that the pair $\left(t, x_2(t)\right)$ at the instant that $x_1(t)$ crosses the zero axis for the first time, belongs to $\mathcal{X}$. From (24), this value is given by

$$x_2(t_1) = x_2(t_0) - \kappa_2 \operatorname{sign}(x_1(t_0))\left[t_1 - t_0\right]. \tag{31}$$

Assume $t_0 = 0$. Then, from the line segments that delimit $\mathcal{X}$ and considering $t = t_1$, κ_2 can be calculated by

$$-\kappa_2(t_c - t_1) \leq x_2(t_1) \leq \kappa_2(t_c - t_1), \tag{32}$$

$$-\kappa_2(t_c - t_1) \leq x_2(t_0) - \kappa_2 \operatorname{sign}(x_1(t_0))t_1 \leq \kappa_2(t_c - t_1), \tag{33}$$

$$-\kappa_2(t_c - t_1) \leq \operatorname{sign}(x_2(t_0))|x_2(t_0)| - \kappa_2 \operatorname{sign}(x_1(t_0))t_1 \leq \kappa_2(t_c - t_1), \tag{34}$$

$$-\kappa_2(t_c - t_1 - \operatorname{sign}(x_1(t_0))t_1) \leq \operatorname{sign}(x_2(t_0))|x_2(t_0)| \leq \kappa_2(t_c - t_1 + \operatorname{sign}(x_1(t_0))t_1), \tag{35}$$

Considering all the possible values that $\operatorname{sign}(x_1(t_0))$ and $\operatorname{sign}(x_2(t_0))$ can assume, one obtains from the previous analysis that

$$\begin{cases} -\kappa_2(t_c - 2t_1) \leq \left|x_2(t_0)\right| \leq \kappa_2 t_c, & \operatorname{sign}(x_1(t_0)) = \operatorname{sign}(x_2(t_0)), \\ -\kappa_2(t_c - 2t_1) \leq -\left|x_2(t_0)\right| \leq \kappa_2 t_c, & \operatorname{sign}(x_1(t_0)) \neq \operatorname{sign}(x_2(t_0)). \end{cases} \tag{36}$$

By choosing a convergence rate $\eta \geq 3$ and κ_2 that satisfies (30), the analytic solution (23) can be solved to find the instant t_1. Equation (36) can be satisfied by either altering the gain κ_2 or the convergence rate η, which directly affects the instant t_1.

Consider now the generalization of (32), to evaluate $x_2(t)$ at every instant that $x_1(t)$ crosses the zero axis. With $j \geq 1$ and $t_j < t_c$, (32) can be rewritten as

$$-\kappa_2(t_c - t_j) \leq x_2(t_j) \leq \kappa_2(t_c - t_j), \tag{37}$$

$$-\kappa_2(t_c - t_j) \leq \operatorname{sign}(x_2(t_0))|x_2(t_0)| - \sum_{m=1}^{j} \kappa_2 \operatorname{sign}(x_1(t_{m-1}))\left[t_m - t_{m-1}\right] \leq \kappa_2(t_c - t_j), \tag{38}$$

where $\operatorname{sign}(x_1(t_{j-1})) = -\operatorname{sign}(x_1(t_j))$. By choosing parameters that satisfy (36), the inequality in (38) is satisfied for every instant t_j obtained from solving (23) for $x_1(t) = 0$. Therefore, a convergence rate $\eta \geq 3$ and a switching gain κ_2 that ensure equations (30) and (36) are satisfied, are sufficient to guarantee that $\left(t, x_2(t)\right) \in \mathcal{X}$, $\forall t \in [t_0, t_c)$. □

The parameter tuning process presented in the proof of Theorem 2 is summarized in Algorithm 1.

Example 1. Consider the system in (21)–(22), with $t_c = 0.5$s, $t_0 = 0$s, $\mathbf{x}(0) = (-2, 1)$, $\kappa_1 = 1$, $\eta = 5$ and $\kappa_2 = 8$. The proposed parameters satisfy (30), but not (36), as illustrated in Fig 3a. From (23), one obtains that $t_1 = 0.2062$s. Using this value to solve (36), the switching gain lower bound is given by $\kappa_2 \geq 11.4155$. Figure 3b shows the trajectory of $x_2(t)$ after adopting $\kappa_2 = 12$. Another way to satisfy (36) is to reduce t_1 by increasing the convergence rate η. The state trajectory obtained by adopting $\eta = 8$ is illustrated in Fig 3c.

Remark 2. It is clear from the definition of $\mathcal{X}$ that its delimiting functions are directly dependent of the switching gain κ_2, which is consequently dependent of the initial value of $x_2(t)$. Therefore, since the system parameters are dependent of the initial conditions of the system, the proposed methodology cannot be defined as fixed-time stable.

Algorithm 1 Modified STA Parameter Tuning

Input: $x_1(t_0)$, $x_2(t_0)$, t_c, t_0, $\eta \geq 3$, $\kappa_2 \geq \frac{|x_2(t_0)|}{t_c - t_0}$
Output: η, κ_2
  $t_1 \leftarrow t \mid x_1(t) = 0$ ▷ Equation (23)
  while $x_2(t_1) \notin \mathcal{X}$ **do** ▷ Equations (31)–(32)
    if $\text{sign}(x_1(t_0)) = \text{sign}(x_2(t_0))$ **then**
      $\kappa_2 \leftarrow \text{floor}\left(\left|\frac{x_2(t_0)}{(t_c - 2t_1)}\right|\right)$ **or** $\eta \leftarrow \eta + 1$
    else
      $\kappa_2 \leftarrow \text{ceil}\left(\left|\frac{x_2(t_0)}{(t_c - 2t_1)}\right|\right)$ **or** $\eta \leftarrow \eta + 1$
    end if
    $t_1 \leftarrow t \mid x_1(t) = 0$
  end while

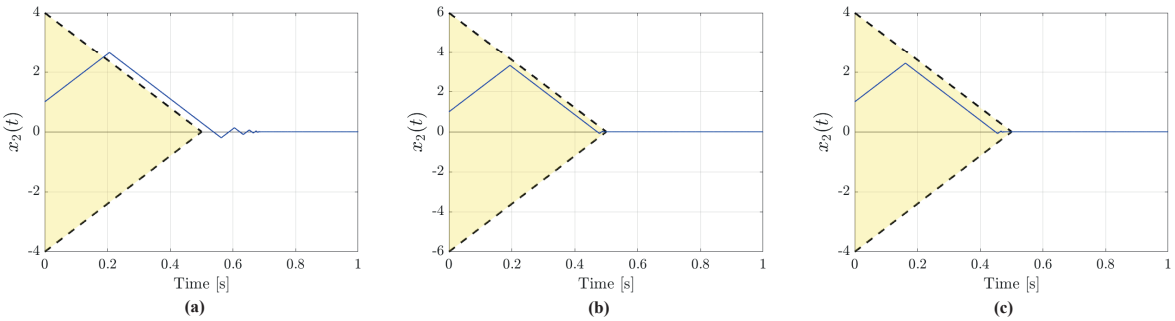

Figure 3: $x_2(t)$ trajectories of the modified STA under different values of η and κ_2, with the PTC area is shaded in yellow. The parameters used in each simulation are (**a**): $\eta = 5$ and $\kappa_2 = 8$, (**b**): $\eta = 5$ and $\kappa_2 = 12$, and (**c**): $\eta = 8$ and $\kappa_2 = 8$.

3.1 | High-gain problem

The proposed stabilizing function contains a term that goes to infinity as t approaches t_c. Nevertheless, the analytic solution in (23) shows that the state $x_1(t)$ approaches the origin as the term is increasing to infinity. However, in an non-ideal scenario, numerical problems such as measurement and discretization errors can cause the state to converge not to the origin, but to a small vicinity of it. This means that the increasing gain $\eta(t_c - t)^{-1}$ will be multiplied by a nonzero value, which causes the state to recede from the origin.

To circumvent this problem, it is possible to alter the instant that the function $\sigma(t, x)$ switches. By employing this solution, the states will not converge to the origin at the switching instant, but to a vicinity of it. Although the property of predefined-time attractiveness of the equilibrium point is lost, convergence to a bounded region around the origin can still be observed.

Corollary 3. For any instant $t_e \in [t_0, t_c)$, the proposed method provides predefined-time convergence of the states to an ultimately bounded region around the origin.

Proof. Consider once again the PTC area $\mathcal{X}$. Assuming the parameters η and κ_2 were sufficiently chosen to provide the predefined-time convergence, the pair $\big(t, x_2(t)\big)$ will remain in $\mathcal{X}$ for all $t \in [t_0, t_c)$. By replacing $x_2(t)$ in (21) by the upper and lower line segments that delimit $\mathcal{X}$, it is possible to obtain functions that delimit a similar bounding region for $x_1(t)$. Denote this set by $\mathcal{Y} = \big\{\big(t, x_1(t)\big) \mid -\xi(t, x, \Omega) \leq x_1(t) \leq \xi(t, x, \Omega)\big\}$, where $\xi(t, x, \Omega)$ is given by

$$\xi(t, x, \Omega) = \frac{\kappa_2(t_c - t)^2}{\eta - 2} + \left(|x_1(t_0)| - \frac{\kappa_2(t_c - t_0)^2}{\eta - 2}\right)\left(\frac{t_c - t}{t_c - t_0}\right)^{\eta}. \tag{39}$$

Therefore, by properly choosing the system parameters, the states will be confined by the bounding regions $\mathcal{X}$ and $\mathcal{Y}$ for any instant $t_e \in [t_0, t_c)$, thus concluding the proof. □

Now assume that $x_1(t)$ is measured with a non-ideal sensor, and (20) for the first finite interval is rewritten as

$$\sigma(t,x) = \frac{\eta}{t_c - t}\check{x}_1(t), \quad t \in [t_0, t_c), \tag{40}$$

$$\check{x}_1(t) \triangleq x_1(t) + \upsilon, \tag{41}$$

where $\upsilon \in \mathbb{R}^n$ is a unknown bounded measurement error, $|\upsilon| \leq \ell$, and ℓ is a positive finite known constant. Considering the worst case scenario, where the minimum value $\left|\check{x}_1(t)\right|$ assumes is ℓ, there will be an instant of time $t_e \in [t_0, t_c)$ when the increasing gain $\eta(t_c - t)^{-1}$ starts to increase the value of $\sigma(t,x)$, instead of reducing it. This instant is obtained by

$$\frac{\eta}{t_c - t_e}\ell = 1, \tag{42}$$

$$t_e = t_c - \eta\ell. \tag{43}$$

Therefore, by altering the proposed function $\sigma(t,x)$ in 24 to

$$\sigma_e(t,x) \triangleq \begin{cases} \frac{\eta}{t_c - t}\check{x}_1(t), & t \in [t_0, t_e), \\ \kappa_1 |\check{x}_1(t)|^{1/2} \operatorname{sign}\left(\check{x}_1(t)\right), & t \in [t_e, \infty), \end{cases} \tag{44}$$

the high-gain problem is avoided. And, since the proposed method drives the states to an ultimately bounded region around the origin, the conventional STA is initialized with finite conditions. However, the predefined-time convergence of the states to the origin at the specified instant of time cannot be guaranteed.

4 | ATTITUDE DETERMINATION PROBLEM

This section proposes an gyroless attitude determination problem to demonstrate an application of the modified STA in the design of state observers. The problem is structured in three phases. The first phase refers to the vehicle's dynamics and sensor measurements. In phase two, an attitude determination method is employed to estimate the vehicle's attitude from the sensor measurements. Finally, in phase three, the estimated attitude is fed to the proposed modified super-twisting observer, to provide estimates of the attitude and its derivative, which will in turn be used to calculate an estimate of the MAV's angular velocity. The framework of this method is illustrated in Figure 4.

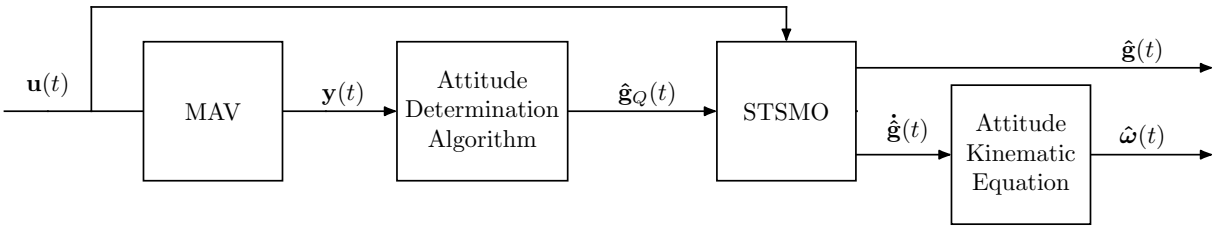

Figure 4: Block diagram representation of the attitude determination problem; $\mathbf{u}(t)$ is the control input, $\mathbf{y}(t)$ is the vector of sensor measurements, $\hat{\mathbf{g}}_Q(t)$ is the attitude estimate from the attitude determination algorithm, represented in Gibbs vector, and $\hat{\mathbf{g}}(t)$, $\dot{\hat{\mathbf{g}}}(t)$ and $\hat{\boldsymbol{\omega}}(t)$ denote, respectively, the attitude estimate, its derivative, and the angular velocity estimate.

The following sections will detail the contents of each phase.

4.1 | Vehicle dynamics and sensor modeling

A Cartesian coordinate system (CCS) with its origin coincident with the MAV's center of mass is defined as $\mathcal{S}^b \triangleq \{B; \vec{x}^{\,b}, \vec{y}^{\,b}, \vec{z}^{\,b}\}$, where B is a point representing its origin, and $\vec{x}^{\,b}$, $\vec{y}^{\,b}$, and $\vec{z}^{\,b}$ are its orthogonal unit vectors, with $\vec{z}^{\,b}$ perpendicular to the rotor plane. Similarly, $\mathcal{S}^g$ represents an inertial CCS with its origin at a reference point fixed on the ground, and its z-axis, $\vec{z}^{\,g}$, aligned with the local vertical. Denote the attitude of $\mathcal{S}^b$ with respect to $\mathcal{S}^g$, represented in Gibbs vector, by $\mathbf{g}^{b/g} \in \mathbb{R}^3$.

This notation can also be abbreviated as $\mathbf{g}$ to avoid notation conflicts with transposition superscripts. The corresponding attitude matrix is given by

$$\mathbf{D}^{b/g}(\mathbf{g}) = \frac{\left(1 - \mathbf{g}^{\mathrm{T}}\mathbf{g}\right)\mathbf{I}_3 + 2\mathbf{g}\mathbf{g}^{\mathrm{T}} - 2\left[\mathbf{g}\times\right]}{1 + \mathbf{g}^{\mathrm{T}}\mathbf{g}}, \tag{45}$$

where $\mathbf{g} = \begin{bmatrix} g_1 & g_2 & g_3 \end{bmatrix}^T$ and $\left[\mathbf{g}\times\right]$ is the following skew-symmetric matrix

$$\left[\mathbf{g}\times\right] \triangleq \begin{bmatrix} 0 & -g_3 & g_2 \\ g_3 & 0 & -g_1 \\ -g_2 & g_1 & 0 \end{bmatrix}. \tag{46}$$

The MAV attitude kinematics are described in terms of the attitude Gibbs vector by

$$\dot{\mathbf{g}}^{b/g} = \frac{1}{2}\mathbf{\Gamma}\left(\mathbf{g}^{b/g}\right)\boldsymbol{\omega}_b^{b/g}, \tag{47}$$

where $\boldsymbol{\omega}_b^{b/g}$ represents the angular velocity of $\mathcal{S}^b$ with respect to $\mathcal{S}^g$ and

$$\mathbf{\Gamma}(\mathbf{g}) \triangleq \mathbf{g}\mathbf{g}^{\mathrm{T}} + \left[\mathbf{g}\times\right] + \mathbf{I}_3. \tag{48}$$

The MAV attitude dynamics can be described by

$$\dot{\boldsymbol{\omega}}_b^{b/g} = \mathbf{J}_b^{-1}\left[(\mathbf{J}_b\,\omega_b^{b/g})\times\right] + \mathbf{J}_b^{-1}\mathbf{u}(t) + \mathbf{J}_b^{-1}\mathbf{d}(t), \tag{49}$$

where $\mathbf{J}_b \in \mathbb{R}^{3\times3}$ is the inertia matrix in $\mathcal{S}^b$, $\mathbf{u}(t) \in \mathbb{R}^3$ is an input torque, and $\mathbf{d}(t) \in \mathbb{R}^3$ is a bounded disturbance torque.

This MAV is equipped with an accelerometer and a magnetometer. The accelerometer measure $\check{\mathbf{a}}_b \in \mathbb{R}^3$ can be modeled by

$$\check{\mathbf{a}}_b = \mathbf{D}^{b/g}\check{\mathbf{a}}_g + \boldsymbol{\delta}_b^{ac}, \quad \text{for} \quad \check{\mathbf{a}}_g \triangleq \dot{\mathbf{v}}_g^{b/g} + g\mathbf{e}_3, \tag{50}$$

where $\check{\mathbf{a}}_g \in \mathbb{R}^3$ is the $\mathcal{S}^g$ representation of the accelerations affecting the MAV, $\dot{\mathbf{v}}_g^{b/g} \in \mathbb{R}^3$ is the $\mathcal{S}^g$ representation of the relative acceleration of $\mathcal{S}^b$ with respect to $\mathcal{S}^r$, $g\mathbf{e}_3 \in \mathbb{R}^3$ is the gravity acceleration vector, and $\boldsymbol{\delta}_b^{ac} \in \mathbb{R}^3$ is a bounded measurement error. To simplify, assume that $\dot{\mathbf{v}}_g^{b/g} = 0$ throughout the experiment. Consequently, $\check{\mathbf{a}}_g$ keeps constant throughout the experiment.

The magnetometer measure $\check{\mathbf{m}}_b \in \mathbb{R}^3$ can be modeled by

$$\check{\mathbf{m}}_b = \mathbf{D}^{b/g}\check{\mathbf{m}}_g + \boldsymbol{\delta}_b^{mg}, \tag{51}$$

where $\check{\mathbf{m}}_g \in \mathbb{R}^3$ is the $\mathcal{S}^g$ representation of the local magnetic field and $\boldsymbol{\delta}_b^{mg} \in \mathbb{R}^3$ is a bounded measurement error. To simplify, assume that $\check{\mathbf{m}}_g$ keeps constant throughout the experiment.

The derivative of equation (48), followed by the substitution of (47) results in

$$\ddot{\mathbf{g}} = \frac{1}{2}\left[\dot{\Gamma}(\mathbf{g})\,\omega_b^{b/g} + \Gamma(\mathbf{g})\left(\mathbf{J}_b^{-1}\left[(\mathbf{J}_b\omega_b^{b/g})\times\right] + \mathbf{J}_b^{-1}\mathbf{u}(t) + \mathbf{J}_b^{-1}\mathbf{d}(t)\right)\right], \tag{52}$$

where $\dot{\Gamma} = \mathbf{g}\dot{\mathbf{g}}^{\mathrm{T}} + \dot{\mathbf{g}}\mathbf{g}^{\mathrm{T}} + \left[\dot{\mathbf{g}}\times\right]$. By defining the states as $\mathbf{x}_1 \triangleq \mathbf{g}$ and $\mathbf{x}_2 \triangleq \dot{\mathbf{g}}$, the system state equations can be written as

$$\dot{\mathbf{x}}_1 = \mathbf{x}_2, \tag{53}$$

$$\dot{\mathbf{x}}_2 = \frac{1}{2}\left[\dot{\Gamma}(\mathbf{g})\,\omega_b^{b/g} + \Gamma(\mathbf{g})\left(\mathbf{J}_b^{-1}\left[(\mathbf{J}_b\omega_b^{b/g})\times\right] + \mathbf{J}_b^{-1}\mathbf{u}(t) + \mathbf{J}_b^{-1}\mathbf{d}(t)\right)\right], \tag{54}$$

$$\mathbf{y} = \begin{bmatrix} \check{\mathbf{a}}_b^{\mathrm{T}} & \check{\mathbf{m}}_b^{\mathrm{T}} \end{bmatrix}^{\mathrm{T}}. \tag{55}$$

4.2 | Attitude estimation

In this phase, the measurements obtained from the available sensors embedded in the vehicle are paired with the measurements taken at the reference CCS to feed the attitude determination algorithm.

A least square estimate of the attitude of a body, represented in quaternion $\hat{\mathbf{q}}(k)$, at instant k can be stated as the minimization of

$$J(\mathbf{q}(k)) = \frac{1}{2}\sum_{i=1}^{n} a_i \|\check{\boldsymbol{\mu}}_b^i(k) - \mathbf{D}(\mathbf{q}(k))\check{\boldsymbol{\mu}}_g^i(k)\|^2, \tag{56}$$

subject to $\|\mathbf{q}(k)\| = 1$, where $\left(\check{\boldsymbol{\mu}}_b^i(k), \check{\boldsymbol{\mu}}_g^i(k)\right)$ is the pair of vector measurements with respect to $\mathcal{S}^b$ and $\mathcal{S}^g$ respectively, $\mathbf{D}(\mathbf{q}(k))$ is the attitude matrix corresponding to the quaternion $\mathbf{q}(k)$, n is the number of vector measurements available at instant k, and a_i is a positive weight associated with the ith measurement pair.

From the work of Shuster and Oh[17], the minimization problem of equation (57) can be replaced by the maximization of

$$G(\mathbf{q}(k)) = \mathbf{q}(k)^{\mathrm{T}}\mathbf{K}(k)\mathbf{q}(k), \tag{57}$$

where

$$\mathbf{K}(k) \triangleq \begin{bmatrix} \mathbf{S}(k) - \varrho(k)\mathbf{I}_3 & \mathbf{z}(k) \\ \mathbf{z}(k)^{\mathrm{T}} & \varrho(k) \end{bmatrix} \in \mathbb{R}^{4\times 4}, \tag{58}$$

$$\mathbf{S}(k) \triangleq \mathbf{B}(k) + \mathbf{B}(k)^{\mathrm{T}} \in \mathbb{R}^{3\times 3}, \tag{59}$$

$$\varrho(k) \triangleq \frac{1}{m(k)} \sum_{i=1}^{n} a_i \breve{\boldsymbol{\mu}}_b^i(k)^{\mathrm{T}} \breve{\boldsymbol{\mu}}_g^i(k) \in \mathbb{R}, \tag{60}$$

$$\mathbf{B}(k) \triangleq \frac{1}{m(k)} \sum_{i=1}^{n} a_i \breve{\boldsymbol{\mu}}_b^i(k) \breve{\boldsymbol{\mu}}_g^i(k)^{\mathrm{T}} \in \mathbb{R}^{3\times 3}, \tag{61}$$

$$\mathbf{z}(k) \triangleq \frac{1}{m(k)} \sum_{i=1}^{n} a_i \left[\breve{\boldsymbol{\mu}}_b^i(k)\times\right] \breve{\boldsymbol{\mu}}_g^i(k) \in \mathbb{R}^3, \tag{62}$$

and

$$m(k) \triangleq \sum_{i=1}^{n} a_i. \tag{63}$$

The solution $\hat{\mathbf{q}}_Q(k)$ to the maximization of $G(\mathbf{q}(k))$ in (57) is given by following eigenvalue/eigenvector equation:

$$\mathbf{K}(k)\hat{\mathbf{q}}_Q(k) = \lambda\hat{\mathbf{q}}_Q(k), \tag{64}$$

where λ is the maximum eigenvalue of $\mathbf{K}(k)$. In other words, the solution $\hat{\mathbf{q}}_Q(k)$ is the eigenvector corresponding to the maximum eigenvalue of $\mathbf{K}(k)$. Shuster and Oh[17] present an efficient algorithm for solving the above eigenvalue/eigenvector problem; this is the well-known QUEST algorithm. The cited work shows that the optimal Gibbs vector[16] is given by

$$\hat{\mathbf{g}}_Q(k) = \left[(\lambda + \varrho(k))\,\mathbf{I}_3 - \mathbf{S}(k)\right]^{-1}\mathbf{z}(k), \tag{65}$$

and the corresponding quaternion is given by

$$\hat{\mathbf{q}}_Q(k) = \frac{1}{\sqrt{\left(1 + \hat{\mathbf{g}}_Q(k)^{\mathrm{T}}\hat{\mathbf{g}}_Q(k)\right)}} \begin{bmatrix} \hat{\mathbf{g}}_Q(k) \\ 1 \end{bmatrix}. \tag{66}$$

4.3 | State observer

Theorem 2 shows that there exist positive parameters that guarantee the finite-time stability with predefined convergence time of the modified STA. Therefore, it is feasible to assign the dynamics of this algorithm to the estimation error, to obtain a finite-time stable observer. Substituting the signum function in equations (21)–(22) for its unit-vector representation results in

$$\dot{\mathbf{x}}_1(t) = -\sigma(t, \mathbf{x}) + \mathbf{x}_2(t), \tag{67}$$

$$\dot{\mathbf{x}}_2(t) = -\kappa_2 \frac{\mathbf{x}_1}{\|\mathbf{x}_1\|} + \boldsymbol{\delta}(t), \tag{68}$$

where

$$\sigma(t, \mathbf{x}) \triangleq \begin{cases} \frac{\eta}{t_c - t}\mathbf{x}_1(t), \ t \in [t_0, t_c), \\ \kappa_1 \frac{\mathbf{x}_1}{\|\mathbf{x}_1\|^{1/2}}, \ t \in [t_c, \infty). \end{cases} \tag{69}$$

Define the estimation error of the states in (53)-(54) as

$$\tilde{\mathbf{x}}_1 \triangleq \mathbf{x}_1 - \hat{\mathbf{x}}_1, \tag{70}$$

$$\tilde{\mathbf{x}}_2 \triangleq \mathbf{x}_2 - \hat{\mathbf{x}}_2, \tag{71}$$

where $\hat{\mathbf{x}}_1$ and $\hat{\mathbf{x}}_2$ are the states estimates. The modified super-twisting algorithm in (76)–(77) can be rewritten as

$$\dot{\tilde{\mathbf{x}}}_1(t) = -\sigma(t, \tilde{\mathbf{x}}) + \tilde{\mathbf{x}}_2(t), \tag{72}$$

$$\dot{\tilde{\mathbf{x}}}_2(t) = -\kappa_2 \frac{\tilde{\mathbf{x}}_1}{\|\tilde{\mathbf{x}}_1\|} + \boldsymbol{\delta}(t), \tag{73}$$

where $\boldsymbol{\delta} \triangleq (f(\mathbf{x}) - f(\hat{\mathbf{x}})) + (b(\mathbf{x}) - b(\hat{\mathbf{x}}))\mathbf{u}(t) + \boldsymbol{\Gamma}(\mathbf{g})\mathbf{d}(t)$ and

$$\sigma(t, \tilde{\mathbf{x}}) \triangleq \begin{cases} \frac{\eta}{t_c - t}\tilde{\mathbf{x}}_1(t), \ t \in [t_0, t_c), \\ \kappa_1 \frac{\tilde{\mathbf{x}}_1}{\|\tilde{\mathbf{x}}_1\|^{1/2}}, \ t \in [t_c, \infty). \end{cases} \tag{74}$$

From equations (53)–(54) and (70)–(71), the following multivariable modified super-twisting sliding mode observer (STSMO) is obtained

$$\dot{\hat{\mathbf{x}}}_1 = \hat{\mathbf{x}}_2 + \sigma(t, \tilde{\mathbf{x}}), \tag{75}$$

$$\dot{\hat{\mathbf{x}}}_2 = \frac{1}{2}\left[\dot{\Gamma}\left(\hat{\mathbf{x}}_1\right)\omega_b^{b/g} + \Gamma\left(\hat{\mathbf{x}}_1\right)\left(\mathbf{J}_b^{-1}\left[(\mathbf{J}_b\omega_b^{b/g})\times\right] + \mathbf{J}_b^{-1}\mathbf{u}(t) + \mathbf{J}_b^{-1}\kappa_2\frac{\tilde{\mathbf{x}}_1}{\|\tilde{\mathbf{x}}_1\|}\right)\right], \tag{76}$$

where $\dot{\Gamma}\left(\hat{\mathbf{x}}_1\right) = \hat{\mathbf{x}}_1\hat{\mathbf{x}}_2^{\mathrm{T}} + \hat{\mathbf{x}}_2\hat{\mathbf{x}}_1^{\mathrm{T}} + \left[\hat{\mathbf{x}}_2\times\right]$ and

$$\sigma(t, \tilde{\mathbf{x}}) \triangleq \begin{cases} \frac{\eta}{t_c - t}\tilde{\mathbf{x}}_1(t), \ t \in [t_0, t_c), \\ \kappa_1 \frac{\tilde{\mathbf{x}}_1}{\|\tilde{\mathbf{x}}_1\|^{1/2}}, \ t \in [t_c, \infty), \end{cases} \tag{77}$$

5 | SIMULATION RESULTS

The simulations in this section were developed in the Matlab software, using the Euler's method of numerical integration, with an integration step $T_s = 0.0001$ s. Consider the following signals

$$\boldsymbol{\omega}_b^{b/g}(t) = \frac{2\pi}{20}\begin{bmatrix} \sin(0.5\pi t) \\ \sin(0.5\pi t + 0.5\pi) \\ \sin(0.5\pi t + \pi) \end{bmatrix}, \qquad \mathbf{d}(t) = 0.05\begin{bmatrix} \sin(50\pi t) \\ \sin(50\pi t + 0.5\pi) \\ \sin(50\pi t + \pi) \end{bmatrix}, \tag{78}$$

where $\boldsymbol{\omega}_b^{b/g}(t)$ is a forcing function acting on equations (54) and (76), and $\mathbf{d}(t)$ is a disturbance torque acting on the system in (53)-(54).

Since the system does not provide a perfect measurement of $\mathbf{x}_1$, the state estimation error described in (70), and used in the observer model in equations (75)–(76), will be rewritten as

$$\tilde{\mathbf{x}}_1 = \hat{\mathbf{g}}_Q(k) - \hat{\mathbf{x}}_1, \tag{79}$$

where $\hat{\mathbf{g}}_Q(k)$ is the optimal Gibbs vector obtained from computing the vector measurements through the QUEST algorithm, using the inverse of the measurement error as the weighting factor a_i. It is possible to see that the existence of measurement error directly affects how close $\hat{\mathbf{g}}_Q(k)$ is to the real attitude vector $\mathbf{g}^{b/g}$. Consequently, $\tilde{\mathbf{x}}_1$ and the observed states will also be affected by the aforementioned error.

After obtaining the estimates $\hat{\mathbf{g}}$ and $\dot{\hat{\mathbf{g}}}$, the attitude kinematic equation (47) is used to compute an angular velocity estimate. Since the matrix $\boldsymbol{\Gamma}(\mathbf{g})$ in equation (48) is non-singular for every $\mathbf{g}$ in this simulation, the MAV angular velocity can be calculated by

$$\boldsymbol{\omega}_b^{b/g} = 2\boldsymbol{\Gamma}^{-1}(\mathbf{g})\dot{\mathbf{g}}, \tag{80}$$

and, inspired by the certainty equivalence principle[57], the angular velocity estimate $\hat{\boldsymbol{\omega}}_b^{b/g}$ can be calculated by (80), by assuming the estimated parameters $\hat{\mathbf{g}}$ and $\dot{\hat{\mathbf{g}}}$ as the real ones. The angular velocity estimation error is given by $\tilde{\boldsymbol{\omega}}_b^{b/g} \triangleq \boldsymbol{\omega}_b^{b/g} - \hat{\boldsymbol{\omega}}_b^{b/g}$.

Initially, consider a perfect measurement of $\breve{\mathbf{a}}_b$ and $\breve{\mathbf{m}}_b$, *i.e.* $\boldsymbol{\delta}_b^{ac} = \boldsymbol{\delta}_b^{mg} = 0$. Using the proposed modified STSMO in (75)–(76), the parameters in Table 1, $\kappa_1 = 1$, $\kappa_2 = 1.5$, and $\eta = 5$, which satisfy the conditions stated in the proof of Theorem 2 for $t_c = 1.5$ s, Figure 5 illustrates the behaviour of the estimation error of $\mathbf{g}$ and $\boldsymbol{\omega}$. Also, Figure 6 reproduces a similar simulation, altering only the predefined convergence instant to $t_c = 0.5$ s, which shows that the chosen parameters are also sufficient to satisfy the stricter time restriction. Even though the provided convergence analyses have considered $\delta(t) = 0$, Figures 5 and 6 illustrate that the proposed algorithm also provides robustness to disturbances.

Table 1: Simulation Parameters.

Symbol	Description	Value
t_f	Simulation Time	3s
Ts	Integration Step	0.0001s
$\boldsymbol{J}$	Inertia Matrix	diag (0.05, 0.05, 0.02) kgm^2
$\mathbf{g}_0$	Initial State	[0.11 0.09 0.11]$^{\mathrm{T}}$
$\hat{\mathbf{g}}_0$	Initial State Estimate	[-0.17 -0.10 0.3]$^{\mathrm{T}}$
$\hat{\mathbf{g}}_0$	Initial State Estimate	[-0.15 0.07 0.11]$^{\mathrm{T}}$
g	Gravity Acceleration	9.81 m/s^2
$\breve{\mathbf{m}}_g$	Local Magnetic Field	[13.7 -4.6 -10.9]$^{\mathrm{T}}$ μT

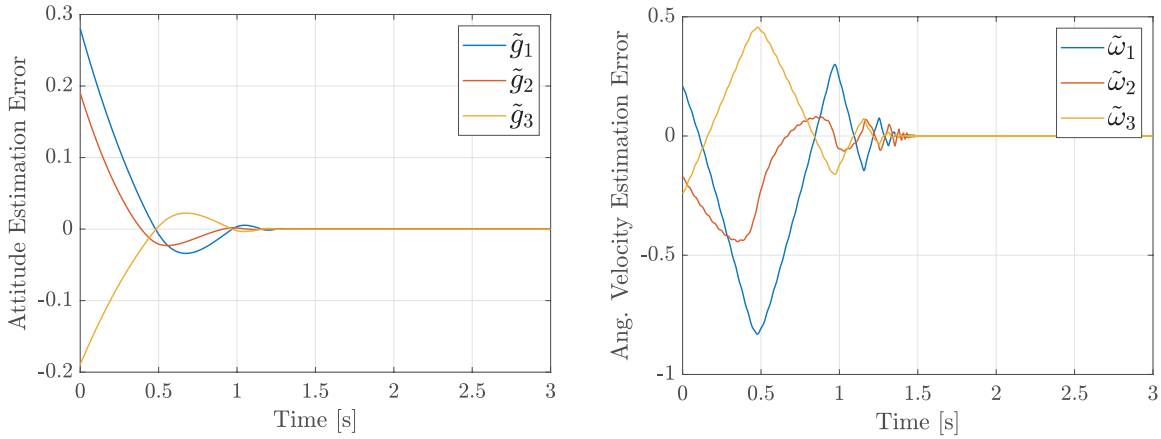

(a) **(b)**

Figure 5: Attitude and angular velocity estimation errors over time, using the proposed modified STSMO, and a predefined convergence instant of $t_c = 1.5$ s.

For the sake of comparison, consider an STSMO designed from the conventional super-twisting algorithm, described by

$$\dot{\hat{\mathbf{x}}}_1 = \hat{\mathbf{x}}_2 + \kappa_1 \frac{\tilde{\mathbf{x}}_1}{\|\tilde{\mathbf{x}}_1\|^{1/2}}, \tag{81}$$

$$\dot{\hat{\mathbf{x}}}_2 = \frac{1}{2}\left[\dot{\Gamma}\left(\hat{\mathbf{x}}_1\right)\omega_b^{b/r} + \Gamma\left(\hat{\mathbf{x}}_1\right)\left(\mathbf{J}_b^{-1}\left[(\mathbf{J}_b\omega_b^{b/r})\times\right] + \mathbf{J}_b^{-1}\mathbf{u}(t) + \mathbf{J}_b^{-1}\kappa_2\frac{\tilde{\mathbf{x}}_1}{\|\tilde{\mathbf{x}}_1\|}\right)\right], \tag{82}$$

where $\dot{\Gamma}\left(\hat{\mathbf{x}}_1\right) = \hat{\mathbf{x}}_1\hat{\mathbf{x}}_2^{\mathrm{T}} + \hat{\mathbf{x}}_2\hat{\mathbf{x}}_1^{\mathrm{T}} + \left[\hat{\mathbf{x}}_2\times\right]$. Using the same parameters from the previous simulation, figures 7a and 7b illustrate the behaviour of the estimation error of $\mathbf{g}$ and $\boldsymbol{\omega}$. It is possible to see that the observer is able to accurately estimate the system's states, even under the influence of a disturbance, driving the estimation error to zero at approximately 1.6s. Unlike the proposed observer, this convergence instant cannot be explicitly chosen and it is directly dependant of the switching gains κ_1 and κ_2 [12].

Now, consider the following bounded noise signals

$$\boldsymbol{\delta}_b^{ac}(t) = 1.5\times10^{-5}\begin{bmatrix}\epsilon\sim\mathcal{U}(-1,1)\\ \epsilon\sim\mathcal{U}(-1,1)\\ \epsilon\sim\mathcal{U}(-1,1)\end{bmatrix}\mathrm{m/s}^2, \tag{83}$$

$$\boldsymbol{\delta}_b^{mg}(t) = 2\times10^{-2}\begin{bmatrix}\epsilon\sim\mathcal{U}(-1,1)\\ \epsilon\sim\mathcal{U}(-1,1)\\ \epsilon\sim\mathcal{U}(-1,1)\end{bmatrix}\mu\mathrm{T}. \tag{84}$$

Using the proposed modified STSMO in (75)–(76), with the parameters in Table 1, $\kappa_1 = 1$, $\kappa_2 = 1.5$, and $\eta = 5$, Figure 8 illustrates the effects of the so-called high-gain problem, addressed in section 3.1. The state $x_1(t)$, when measured with non-ideal sensors, does not converge exactly to zero, but to a bounded neighborhood of zero. So, when t approaches t_c, the time-varying

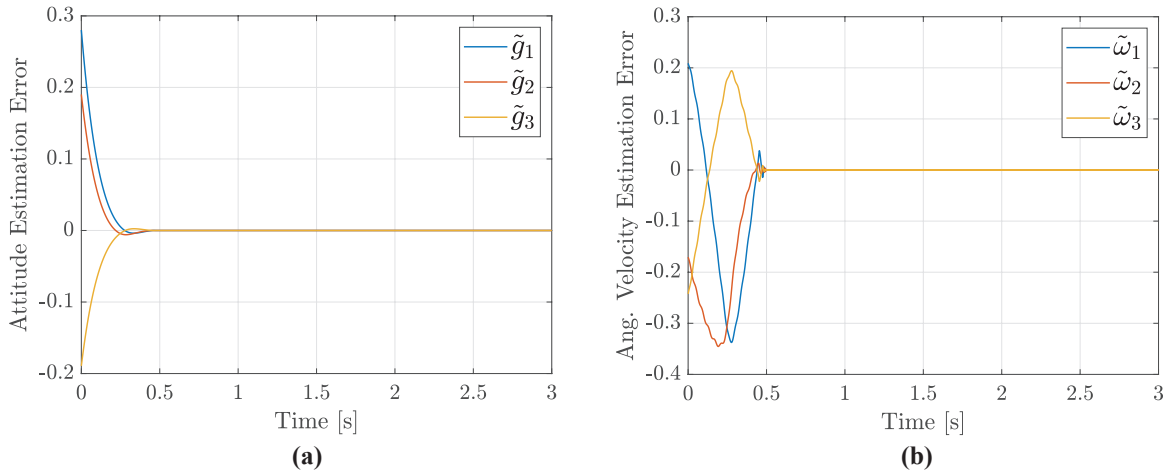

Figure 6: Attitude and angular velocity estimation errors over time, using the proposed modified STSMO, and a predefined convergence instant of $t_c = 0.5$ s.

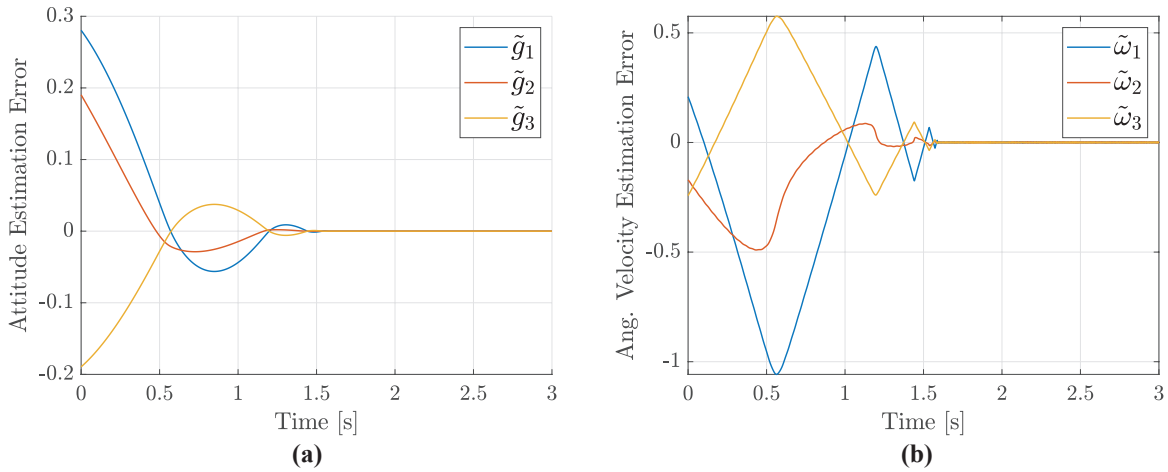

Figure 7: Attitude and angular velocity estimation errors over time, using a conventional super-twisting sliding-mode observer.

gain $\eta(t_c - t)^{-1}$ approaches infinity and it multiplies a non-zero state, which causes the departure from the origin in Figures 8a–8b. As proposed, it is possible to avoid this problem by switching the σ-function in (77) earlier.

From equations (83)–(84), it is possible to calculate an upper bound to the measurement error at $\|\boldsymbol{\delta}(t)\| \leq 0.0346$. By using this bound and the system parameters, equation (43) gives an earlier switching instant of $t_e = 1.3268$ s. Figure 9 illustrates the behaviour of the estimation errors, using a earlier switching instant.

6 | CONCLUSIONS

The conventional super-twisting algorithm (STA) does not provide to the user an explicit convergence instant, nor can it be easily calculated from its switching gains. Theorems that prove the algorithm's finite-time stability only specify an upper bound for the reaching time, but cannot pinpoint the exact instant of convergence. With the proper choice of the parameters in the vector $\boldsymbol{\Omega}$, the proposed modified STA provides the desired finite-time stability with predefined convergence time, as verified by the simulations. Also, by sacrificing exactness of convergence time, it is possible to avoid the high-gain problem which appears in non-ideal scenarios involving predefined-time convergence. Additionally, a multivariable super-twisting sliding mode observer,

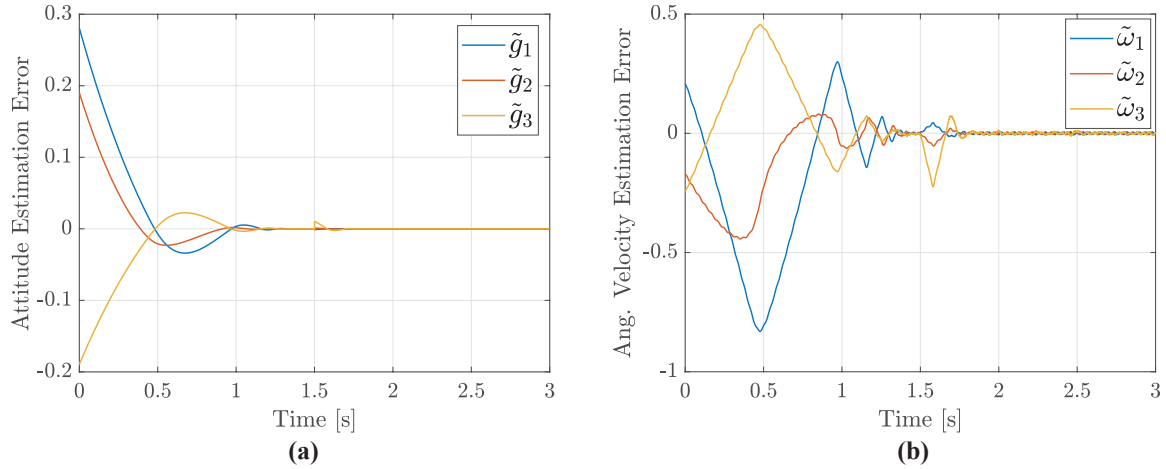

Figure 8: Attitude and angular velocity estimation errors over time under the influence of measurement noise, using the proposed modified super-twisting sliding-mode observer with a predefined convergence instant of $t_c = 1.5$ s.

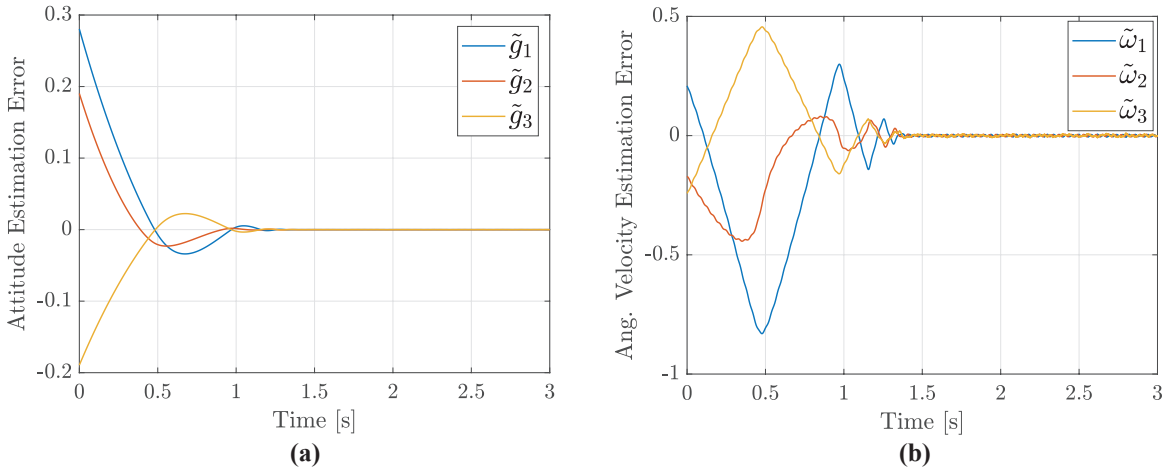

Figure 9: Attitude and angular velocity estimation errors over time under the influence of measurement noise, using the proposed modified super-twisting sliding-mode observer with a predefined convergence instant of $t_c = 1.5$ s, and an earlier switching time of $t_e = 1.3268$ s.

created from the proposed modified STA, was employed to estimate the attitude and the angular velocity of a multirotor aerial vehicle. This observer has shown to provide a robust and accurate estimation of the vehicle rotational states, while also allowing a straightforward performance tweaking by altering the predefined convergence time, demonstrating its increased versatility in comparison to the conventional super-twisting observer.

References

1. Levant A. Sliding order and sliding accuracy in sliding mode control. *International Journal of Control* 1993; 58(6): 1247–1263. doi: 10.1080/00207179308923053

2. Moreno JA, Osorio M. Strict Lyapunov functions for the super-twisting algorithm. *IEEE Transactions on Automatic Control* 2012; 57(4): 1035–1040. doi: 10.1109/tac.2012.2186179

3. Davila J, Fridman L, Levant A. Second-order sliding-mode observer for Mechanical Systems. *IEEE Transactions on Automatic Control* 2005; 50(11): 1785–1789. doi: 10.1109/tac.2005.858636

4. Kommuri SK, Han S, Lee S. External torque estimation using higher order sliding-mode observer for robot manipulators. *IEEE/ASME Transactions on Mechatronics* 2022; 27(1): 513–523. doi: 10.1109/tmech.2021.3067443

5. Castaneda H, Salas-Pena OS, Leon Morales dJ. Adaptive Super Twisting Flight Control-observer for a fixed wing UAV. *2013 International Conference on Unmanned Aircraft Systems (ICUAS)* 2013. doi: 10.1109/icuas.2013.6564788

6. Silva JF, Santos DA. Attitude determination for multirotor aerial vehicle using a super-twisting sliding mode observer. *26th International Congress of Mechanical Engineering (COBEM)* 2021.

7. Andrieu V, Praly L, Astolfi A. Homogeneous approximation, recursive observer design, and output feedback. *SIAM Journal on Control and Optimization* 2008; 47(4): 1814–1850. doi: 10.1137/060675861

8. Polyakov A. Nonlinear feedback design for fixed-time stabilization of linear control systems. *IEEE Transactions on Automatic Control* 2012; 57(8): 2106–2110. doi: 10.1109/tac.2011.2179869

9. Holloway J, Krstic M. Prescribed-time observers for linear systems in observer canonical form. *IEEE Transactions on Automatic Control* 2019; 64(9): 3905–3912. doi: 10.1109/tac.2018.2890751

10. Davila A, Moreno JA, Fridman L. Optimal lyapunov function selection for reaching time estimation of super twisting algorithm. *Proceedings of the 48h IEEE Conference on Decision and Control (CDC) held jointly with 2009 28th Chinese Control Conference* 2009. doi: 10.1109/cdc.2009.5400466

11. Polyakov A, Poznyak A. Reaching time estimation for "super-twisting" Second order sliding mode controller via Lyapunov function designing. *IEEE Transactions on Automatic Control* 2009; 54(8): 1951–1955. doi: 10.1109/tac.2009.2023781

12. Seeber R, Horn M, Fridman L. A novel method to estimate the reaching time of the super-twisting algorithm. *IEEE Transactions on Automatic Control* 2018; 63(12): 4301–4308. doi: 10.1109/tac.2018.2812789

13. Cruz-Zavala E, Moreno JA, Fridman LM. Uniform robust exact differentiator. *IEEE Transactions on Automatic Control* 2011; 56(11): 2727–2733. doi: 10.1109/tac.2011.2160030

14. Seeber R, Haimovich H, Horn M, Fridman LM, De Battista H. Robust exact differentiators with predefined convergence time. *Automatica* 2021; 134: 109858. doi: 10.1016/j.automatica.2021.109858

15. Wahba G. A Least Squares Estimate of Satellite Attitude. *SIAM Review* 1965; 7(3): 409–409. doi: 10.1137/1007077

16. Wertz JP. *Spacecraft attitude determination and control*. Kluwer . 1978.

17. Shuster MD, Oh SD. Three-axis attitude determination from vector observations. *Journal of Guidance and Control* 1981; 4(1): 70–77. doi: 10.2514/3.19717

18. Reynolds RG. Quaternion parameterization and a simple algorithm for global attitude estimation. *Journal of Guidance, Control, and Dynamics* 1998; 21(4): 669–672. doi: 10.2514/2.4290

19. Markley F. Fast quaternion attitude estimation from two vector measurements. *Journal of Guidance, Control, and Dynamics* 2002; 25(2): 411–414. doi: 10.2514/2.4897

20. Lefferts E, Markley F, Shuster M. Kalman filtering for spacecraft attitude estimation. *20th Aerospace Sciences Meeting* 1982. doi: 10.2514/6.1982-70

21. Bar-Itzhack IY. REQUEST - A recursive QUEST algorithm for sequential attitude determination. *Astrodynamics Conference* 1996. doi: 10.2514/6.1996-3617

22. Bar-Itzhack IY, Idan M. Recursive attitude determination from vector observations Euler angle estimation. *Journal of Guidance, Control, and Dynamics* 1987; 10(2): 152–157. doi: 10.2514/3.22911

23. Bar-Itzhack IY, Oshman Y. Attitude Determination from Vector Observations: Quaternion Estimation. *IEEE Transactions on Aerospace and Electronic Systems* 1985; AES-21(1): 128–136. doi: 10.1109/taes.1985.310546

24. Bar-Itzhack IY, Reiner P. Recursive Attitude Determination from Vector Observations: Direction Cosine Matrix Identification. *Journal of Guidance, Control, and Dynamics* 1984; 7(1): 51–56. doi: 10.2514/3.56362

25. Markley FL. Attitude Determination And Parameter Estimation Using Vector Observations: Theory. *The Journal of Astronautical Sciences* 1989; 37(1): 41–58.

26. Markley FL, Crassidis JL. *Fundamentals of spacecraft attitude determination and control*. Springer . 2014.

27. Psiaki ML, Martel F, Pal PK. Three-axis attitude determination via Kalman filtering of magnetometer data. *Journal of Guidance, Control, and Dynamics* 1990; 13(3): 506–514. doi: 10.2514/3.25364

28. Lizarralde F, Wen J. Attitude control without angular velocity measurement: A passivity approach. *Proceedings of 1995 IEEE International Conference on Robotics and Automation* 1995. doi: 10.1109/robot.1995.525665

29. Bar-Itzhack IY. Classification of algorithms for angular velocity estimation. *Journal of Guidance, Control, and Dynamics* 2001; 24(2): 214–218. doi: 10.2514/2.4731

30. Carmi A, Oshman Y. Vector observations-based gyroless spacecraft attitude/angular rate estimation using particle filtering. *AIAA Guidance, Navigation, and Control Conference and Exhibit* 2006. doi: 10.2514/6.2006-6597

31. Ma H, Xu S. Magnetometer-only attitude and angular velocity filtering estimation for attitude changing spacecraft. *Acta Astronautica* 2014; 102: 89–102. doi: 10.1016/j.actaastro.2014.05.002

32. Hajiyev C. Review on gyroless attitude determination methods for small satellites. *Progress in Aerospace Sciences* 2017; 90: 54–66. doi: 10.1016/j.paerosci.2017.03.003

33. Zhang PF, Hao JH, Chen Q. Gyro-less angular velocity estimation and intermittent attitude control of spacecraft using coarse-sensors based on geometric analysis. *Aerospace Science and Technology* 2020; 103: 105900. doi: 10.1016/j.ast.2020.105900

34. Martin P, Salaün E. Design and implementation of a low-cost observer-based attitude and heading reference system. *Control Engineering Practice* 2010; 18(7): 712–722. doi: 10.1016/j.conengprac.2010.01.012

35. Magnussen O, Ottestad M, Hovland G. Experimental validation of a quaternion-based attitude estimation with direct input to a Quadcopter Control System. *2013 International Conference on Unmanned Aircraft Systems (ICUAS)* 2013. doi: 10.1109/icuas.2013.6564723

36. Mahony R, Hamel T, Pflimlin JM. Nonlinear complementary filters on the Special Orthogonal Group. *IEEE Transactions on Automatic Control* 2008; 53(5): 1203–1218. doi: 10.1109/tac.2008.923738

37. Mahony R, Kumar V, Corke P. Multirotor Aerial Vehicles: Modeling, estimation, and control of Quadrotor. *IEEE Robotics & Automation Magazine* 2012; 19(3): 20–32. doi: 10.1109/mra.2012.2206474

38. Hua MD, Ducard G, Hamel T, Mahony R, Rudin K. Implementation of a nonlinear attitude estimator for aerial robotic vehicles. *IEEE Transactions on Control Systems Technology* 2014; 22(1): 201–213. doi: 10.1109/tcst.2013.2251635

39. Zhang ZQ, Meng XL, Wu JK. Quaternion-based Kalman filter with vector selection for accurate orientation tracking. *IEEE Transactions on Instrumentation and Measurement* 2012; 61(10): 2817–2824. doi: 10.1109/tim.2012.2196397

40. Rigatos GG. Nonlinear Kalman filters and particle filters for integrated navigation of Unmanned Aerial Vehicles. *Robotics and Autonomous Systems* 2012; 60(7): 978–995. doi: 10.1016/j.robot.2012.03.001

41. Sebesta KD, Boizot N. A real-time adaptive high-gain EKF, applied to a quadcopter inertial navigation system. *IEEE Transactions on Industrial Electronics* 2014; 61(1): 495–503. doi: 10.1109/tie.2013.2253063

42. Santos DA, Gonçalves PFSM. Attitude Determination of Multirotor Aerial Vehicles Using Camera Vector Measurements. *Journal of Intelligent & Robotic Systems* 2016; 86(1): 139–149. doi: 10.1007/s10846-016-0418-0

43. Gośliński J, Giernacki W, Królikowski A. A nonlinear filter for efficient attitude estimation of Unmanned Aerial Vehicle (UAV). *Journal of Intelligent & Robotic Systems* 2018; 95(3-4): 1079–1095. doi: 10.1007/s10846-018-0949-7

44. Ma HJ, Liu Y, Li T, Yang GH. Nonlinear high-gain observer-based diagnosis and compensation for actuator and sensor faults in a quadrotor unmanned aerial vehicle. *IEEE Transactions on Industrial Informatics* 2019; 15(1): 550–562. doi: 10.1109/tii.2018.2865522

45. Benallegue A, Mokhtari A, Fridman L. High-order sliding-mode observer for a quadrotor UAV. *International Journal of Robust and Nonlinear Control* 2008; 18(4-5): 427–440. doi: 10.1002/rnc.1225

46. El Hadri A, Benallegue A. Sliding mode observer to estimate both the attitude and the gyro-bias by using low-cost sensors. *2009 IEEE/RSJ International Conference on Intelligent Robots and Systems* 2009. doi: 10.1109/iros.2009.5353974

47. Ahmad I, Benallegue A, El Hadri A. Sliding mode based attitude estimation for accelerated aerial vehicles using GPS/IMU measurements. *2013 IEEE International Conference on Robotics and Automation* 2013. doi: 10.1109/icra.2013.6631014

48. Chang J, Cieslak J, Davila J, Zolghadri A, Zhou J. Adaptive second-order sliding mode observer for Quadrotor Attitude Estimation. *2016 American Control Conference (ACC)* 2016. doi: 10.1109/acc.2016.7525252

49. Sanchez-Torres JD, Sanchez EN, Loukianov AG. Predefined-time stability of dynamical systems with sliding modes. *2015 American Control Conference (ACC)* 2015. doi: 10.1109/acc.2015.7172255

50. Jimenez-Rodriguez E, Sanchez-Torres JD, Gomez-Gutierrez D, Loukianov AG. Predefined-time tracking of a class of mechanical systems. *2016 13th International Conference on Electrical Engineering, Computing Science and Automatic Control (CCE)* 2016. doi: 10.1109/iceee.2016.7751197

51. Song Y, Wang Y, Holloway J, Krstic M. Time-varying feedback for regulation of normal-form nonlinear systems in prescribed finite time. *Automatica* 2017; 83: 243–251. doi: 10.1016/j.automatica.2017.06.008

52. Agarwal RP, Lakshmikantham V. *Uniqueness and nonuniqueness criteria for ordinary differential equations*. World Scientific . 1993.

53. Nagesh I, Edwards C. A multivariable super-twisting sliding mode approach. *Automatica* 2014; 50(3): 984–988. doi: 10.1016/j.automatica.2013.12.032

54. Filippov AF. *Differential equations with: Discontinuous righthand sides*. Kluwer Academic Pubr. . 1989.

55. Moulay E, Perruquetti W. Finite time stability conditions for non-autonomous continuous systems. *International Journal of Control* 2008; 81(5): 797–803. doi: 10.1080/00207170701650303

56. Seeber R, Horn M. Stability proof for a well-established super-twisting parameter setting. *Automatica* 2017; 84: 241–243. doi: 10.1016/j.automatica.2017.07.002

57. Water dHV, Willems J. The certainty equivalence property in stochastic control theory. *IEEE Transactions on Automatic Control* 1981; 26(5): 1080–1087. doi: 10.1109/tac.1981.1102781

How to cite this article: J.F. Silva, and D.A. Santos (2022), Attitude and Angular Velocity Estimation for Multirotor Aerial Vehicles using a Modified Super-Twisting Algorithm with Predefined Convergence Time, *Int J Robust Nonlinear Control*, ….